

Efficient Bayesian species tree inference under the multi-species coalescent

Bruce Rannala¹ and Ziheng Yang²

¹Department of Evolution & Ecology, University of California, Davis, CA 95616, USA

²Department of Genetics, Evolution and Environment, University College London, London WC1E 6BT, UK

Keywords: Bayesian inference — species tree — multi-species coalescent — MCMC — SPR — nodeslider

Correspondence to:

Ziheng Yang

Department of Genetics, Evolution and Environment, University College London, London WC1E 6BT, UK

Phone: 020 7679 4379

Email: z.yang@ucl.ac.uk

Running Head: Bayesian species tree inference

Abstract

A method was developed for Bayesian inference of species phylogeny using the multi-species coalescent model. To improve the mixing properties of the Markov chain Monte Carlo (MCMC) algorithm that traverses the space of species trees, we implement two efficient MCMC proposals: the first is based on the Subtree Pruning and Regrafting (SPR) algorithm and the second is based on a novel node-slider algorithm. Like the Nearest-Neighbor Interchange (NNI) algorithm we implemented previously, both algorithms propose changes to the species tree, while simultaneously altering the gene trees at multiple genetic loci to automatically avoid conflicts with the newly-proposed species tree. The method integrates over gene trees, naturally taking account of the uncertainty of gene tree topology and branch lengths given the sequence data. A simulation study was performed to examine the statistical properties of the new method. We found that it has excellent statistical performance, inferring the correct species tree with near certainty when analyzing 10 loci. The prior on species trees has some impact, particularly for small numbers of loci. An empirical dataset (for rattlesnakes) was reanalyzed. While the 18 nuclear loci and one mitochondrial locus support largely consistent species trees under the multi-species coalescent model estimates of parameters suggest drastically different evolutionary dynamics between the nuclear and mitochondrial loci.

Introduction

Multilocus genetic sequence data have gained importance in inferring species trees in recent years and several inference methods have been proposed for this purpose. As noted by Maddison (1997) several processes can cause the species tree to differ from gene trees underlying particular loci. Some of these processes, such as introgression between species and horizontal gene transfer, involve reticulations in the species tree, whereas others, such as incomplete lineage sorting and gene duplications, occur within the context of a non-reticulate (and typically binary) species tree. An important potential source of gene-tree versus species-tree conflicts among genetically isolated species is incomplete lineage sorting; this phenomenon is typically modeled using a coalescence process. A simple widely-used method for multilocus species tree inference concatenates sequences from different loci, assuming that a single tree (treated as the species tree) underlies all the loci (reviewed in Rannala and Yang, 2008; Edwards, 2009). This approach can lead to strongly supported incorrect phylogenetic trees when incomplete lineage sorting occurs (see e.g., Leaché and Rannala, 2011), and has been shown to be inconsistent (Kubatko and Degnan, 2007). Another heuristic approach is to infer separate gene trees and then attempt to reconcile the differences among gene trees to obtain an estimate of the species tree (Page and Charleston, 1997). Use of the most frequent gene tree among loci as the species tree estimate can be inconsistent in the so-called 'anomaly zone' (Degnan and Salter, 2005; Degnan and Rosenberg, 2006).

Maddison (1997) and Maddison and Knowles (2006) proposed a parsimony-inspired method for inferring the species tree called minimizing deep coalescence (MDC) events for gene trees. Other examples include species tree estimation by minimizing coalescence times across genes (the Global LAteSt Split, GLASS; Mossel and Roch, 2010), by using the average ranks of coalescences (STAR; Liu *et al.*, 2009), by using average coalescence times (STEAC; Liu *et al.*, 2009), by using maximum likelihood for gene trees under coalescence (STEM; Kubatko *et al.*, 2009) and by maximum pseudo-likelihood (M-PEST; Liu *et al.*, 2010). These approximations treat the estimated gene trees (including either the gene tree topology alone or both the gene tree topology and branch lengths) as observations (data), ignoring phylogenetic uncertainties. Such approximations can lead to systematic biases as well as underestimation of the uncertainty of inferred species trees (Leaché and Rannala, 2011).

A parametric statistical method for inferring the species tree using multi-locus sequence data should integrate over the (unobserved) gene trees (both the tree topology and branch lengths). For the case of three species, with one sequence from each species at each locus, a maximum likelihood method was implemented by Yang (2002), using numerical integration to integrate out the two coalescent times in each gene tree. For larger problems with more species or more sequences, maximum likelihood is not computationally feasible.

Instead the Bayesian method is used, with Markov chain Monte Carlo (MCMC) used for the computation. A few MCMC implementations now exist to estimate species trees (Edwards *et al.*, 2007; Heled and Drummond, 2010; Ronquist *et al.*, 2012) although they are limited to a small number of species and loci.

The mutual constraints imposed by the gene trees and the species tree are a challenge for developing an efficient MCMC inference program under the multi-species coalescent model. For example, if the divergence time between species A and B is τ_{AB} , the divergence time between two sequences from A and B must be older with $t_{AB} > \tau_{AB}$ at every locus (sequences must diverge before the species diverge). Such constraints can cause serious difficulties leading to poor MCMC mixing when one attempts to change species divergence times and/or the species tree topology if the gene trees are fixed. There are two possible solutions to this difficulty: either analytically integrate over the gene trees (rather than performing MCMC) preserving the constraints; or develop efficient MCMC proposals for jointly modifying the species tree and the gene trees that obey the constraints. Recent methods that have been developed for inferring species trees from single nucleotide polymorphism (SNP) data follow the first strategy (Bryant *et al.*, 2012). The simplicity of these data allow the gene trees to be analytically integrated out of the model. However, a drawback of such methods is that SNPs provide very little information about branch lengths in the gene trees and the power is therefore expected to be reduced in comparison with sequence-based methods.

Here, we follow the second approach in developing a Bayesian inference procedure for the analysis of multi-locus sequence data that jointly infers the species phylogeny and gene trees as well as other relevant parameters such as ancestral population sizes and species divergence times. We extend our program BPP (for Bayesian Phylogenetics and Phylogeography) (Yang and Rannala, 2010; Rannala and Yang, 2013; Yang and Rannala, 2014) to allow this joint inference. We develop two novel MCMC proposals to change the species tree, at the same time modifying the gene trees to avoid conflicts between the gene trees and newly proposed species tree. The first move is based on the Subtree Pruning and Regrafting (SPR) algorithm for rooted trees. This changes the species tree topology while preserving the node ages in the species tree as well as in the gene trees. The second move is based on a node-slider algorithm, which changes the topology as well as the node ages in the species tree and gene trees. The two new proposal algorithms lead to greatly improved mixing behavior of the MCMC by comparison with the simple NNI algorithm implemented in our previous work (Yang and Rannala, 2014).

Theory

Here we review the formulation of the species tree inference problem in a Bayesian framework and then describe our new MCMC algorithms. Let X_i be the sequence alignment for locus i . The number of sequences per species may vary for each locus and some species may not be sampled for a particular locus. Our requirement is that every locus should have at least two sequences. Let there be L loci and define $\mathbf{X} = \{X_i\}$ to be the full dataset. Let G_i be the gene tree for the sequences sampled at locus i (including both the gene tree topology and branch lengths or coalescent times). Let $\mathbf{G} = \{G_i\}$. We assume the loci are unlinked so that

$$f(\mathbf{X}|\mathbf{G}, \omega) = \prod_{i=1}^L f(X_i|G_i, \omega). \quad (1)$$

where $f(X_i|G_i, \omega)$ is the *phylogenetic likelihood* calculated according to the usual Felsenstein algorithm (Felsenstein, 1981) and ω is a vector of parameters in the nucleotide substitution model. The posterior probability of the species tree (S) and the parameters is given by

$$f(S, \Theta|\mathbf{X}) = \frac{1}{f(\mathbf{X})} \int_{\omega} \int_G f(\mathbf{X}|\mathbf{G}, \omega) f(\mathbf{G}|S, \Theta) f(\omega) f(\Theta) f(S) d\mathbf{G}d\omega, \quad (2)$$

where $\Theta = \{\{\tau_j\}, \{\theta_j\}\}$ is the set of θ s and τ s associated with the species tree(s). Note that $\theta_j = 4N_j\mu$ where N_j is the effective population size of (ancestral or contemporary) species j . The branch lengths in the gene trees and the divergence times in the species trees are represented in units of expected number of substitutions

per site (as in Rannala and Yang, 2003). The term $f(\mathbf{G}|S, \Theta)$ is the multispecies coalescent density of gene trees (topology and coalescent times) given the species tree (Rannala and Yang, 2003). We use MCMC to generate a sample from the posterior density of S and Θ . Here we focus on two new MCMC proposals that efficiently propose changes to the species tree topology (S). The moves that do not alter the species tree topology are identical to those described in Rannala and Yang (2003, 2013). The first move, based on the SPR algorithm, is a direct extension of the Nearest-Neighbor Interchange (NNI) algorithm implemented in Yang and Rannala (2014). The second move, based on a node-slider algorithm, changes the topology as well as a node age in the species tree.

SPR algorithm to modify the species tree topology

Let $\text{anc}(a)$ be the mother node of node a . We refer to the branch $\text{anc}(a)$ - a as branch a . We define clade or subtree a to include a , all its descendants, and branch a . Nodes on the species tree are represented by capital letters, such as A , and their ages are denoted by τ s (such as τ_A). Nodes on gene trees are labeled using small-case letters, and their ages are denoted by ts .

Our SPR move prunes off the branch Y - A (including clade A) and reattaches it to a target branch C , retaining the same age τ_Y at reattachment (fig. 1). Our algorithm does not change divergence times (τ s) in the species tree or node ages (ts) in the gene trees. We preferentially propose changes to the species tree topology around short (rather than long) internal branches. We sample an internal branch i (out of $s - 2$ internal branches for a species tree of s species) according to the following probabilities

$$w_i \propto b_i^{-\frac{1}{2}}, \quad (3)$$

where b_i is the length of the internal branch. The sampled branch is branch X - Y . Node Y has two daughter branches. We sample one at random and let it be A ; the other will be B . We then prune off branch Y - A (including clade A) and reattach it to branch C in the species tree. Let Z be the most recent common ancestor of A and C , with age τ_Z . The move affects species on the path A - Z - C . For the SPR move illustrated in fig. 1, Y is species AB , X is ABD , and Z is $ABCD$.

Among the feasible target branches for reattachment, we sample one using a probability distribution that favors small changes to the species tree topology. A feasible target branch is a branch of the species tree that remains after branch Y - A is pruned off (exclusive of branch B) and that covers the age τ_Y (see fig. 1). In choosing a target branch, we use probabilities

$$v_i \propto 1/c_i, \quad (4)$$

where c_i is the number of nodes on the path A - Z - C_i for potential target branch C_i . The minimum for c_i is 3, in which case $Z = X$ and the SPR move reduces to the NNI move of Yang and Rannala (2014). Our proposal using equation 4 thus favours small changes to the species tree topology.

The move affects nodes on the gene trees that have age $\tau_Y < t < \tau_Z$. A *moved* node (marked with \bullet in fig. 1) lies in species AB (Y) or another ancestral species on the path from Y to Z (excluding Z itself) and has exactly one daughter node with descendants in A only. The other daughter node has descendants in one or more non- A descendent populations as well. The moved node (and the descendant clade) is pruned and re-grafted to a randomly chosen contemporary branch of the gene tree residing in a species on the path from C to Z . In addition, four other kinds of *affected* nodes have their population IDs changed. Any node marked with \circ or \triangle has descendants in species A only and changes its population ID from AB (Y) to AC . Any node marked with \diamond is in species C with age between τ_Y and $\tau_{\text{anc}(C)}$ and changes its population ID from C to AC . Any node marked with \square is in species AB with both daughter nodes having descendants in species B , and changes its population ID from AB to B . The proposal ratio incurred by the move can be easily derived using a procedure similar to that used for the NNI move (Yang and Rannala, 2014)

Nodeslider algorithm to modify the species tree

Overview of the algorithm

The nodeslider move prunes off branch $Y-A$ (including clade A) in the species tree, changes τ_Y and rescales the ages inside the A clade proportionally, and then reattaches the branch (and the A clade) to a new branch C in the remaining species tree (fig. 2). This proposal consists of a pair of opposing moves, referred to as the ‘Expand’ and ‘Shrink’ moves. In the Expand move (towards the root), τ_Y increases, and the target branch C is ancestral to node Y . In the Shrink move (towards the tips), τ_Y decreases, and the target branch C is one of the descendants of B , the sibling of A . Thus the move slides node Y and the attached clade A either towards the root, with the node ages in subtree A expanded, or to a descendent branch of the sibling species B , with the node ages in subtree A shrunk.

Details of the algorithm

1. Changes to the species tree: We describe the changes to the species tree first. A uniform random variable U on $(0, 1)$ is generated to decide whether to expand ($U \geq 0.5$) or shrink ($U < 0.5$). In the Expand move (change from S to S^* in fig. 2), we use equation 3 to sample an internal branch (out of $s - 2$) on the species tree and let it be $X-Y$. Node Y has two daughter nodes. We sample one at random and let it be A ; the other will be B . In the example of fig. 2, X is node 6, and Y is node 7. We then propose a new age τ_Y^* for node Y using an exponential density,

$$f(\tau_Y^*) = \left(\frac{1}{0.1\tau_X} \right) e^{-\frac{1}{0.1\tau_X}(\tau_Y^* - \tau_X)}, \quad \tau_X < \tau_Y^* < \infty. \quad (5)$$

In other words, the excess $\tau_Y^* - \tau_X$ has mean $0.1\tau_X$. The value 0.1 is the ‘‘Expand ratio’’ and is adjustable; we suspect small values close to zero are preferable. Branch $Y-A$ (including clade A) is pruned off and reattached to the remaining species tree at age τ_Y^* . There will be only one ancestral branch which covers the new age τ_Y^* . Note that this can be the root, in which case node Y will become the new root.

In the Shrink move, we use equation 3 to sample an internal branch on the species tree and let it be $Y-B$. The other daughter of node Y (that is, the sibling of B) will be A . Branch $Y-A$ (including clade A) will be pruned off and reattached to a target branch C that is a descendent of species B at time τ_Y^* . The new age τ_Y^* is proposed using a power density,

$$f(\tau_Y^*) = \frac{\lambda}{\tau_B} \left(\frac{\tau_Y^*}{\tau_B} \right)^{\lambda-1}, \quad 0 < \tau_Y^* < \tau_B. \quad (6)$$

This is a uniform density if $\lambda = 1$. To simulate from the power density we use the inverse transformation method. Generate a uniform random variable $u \sim U(0, 1)$ and set

$$\tau_Y^* = \tau_B \times u^{1/\lambda}. \quad (7)$$

We choose $\lambda = \log(0.1)/\log(0.9) = 21.85$ so that 90% of the density is within 10% of τ_B , with $\tau_Y^* \geq 0.9 \times \tau_B$. Here the value 10% is called the ‘‘Shrink ratio.’’ We favor small values like 10% so that the new τ_Y^* , smaller than τ_B , tends to be close to it.

When branch $Y-A$ is pruned off, the ages of all daughter nodes of A are rescaled by the factor τ_Y^*/τ_Y . In the Expand move, we slide branch $Y-A$ (including clade A) towards the root. We find the branch ancestral to X at age τ_Y^* for reattachment. In the Shrink move, we select a branch at random as target for reattachment, among all branches that are descendants of B and exist at time point τ_Y^* . The number of branches for reattachment is 1 in the Expand move, and is greater than 1 in the Shrink move.

We now consider the factor in the proposal ratio incurred by changes to the species tree. First, consider the Shrink move (e.g., $S^* \rightarrow S$ in fig. 2). Let $G(\tau_Y^*)$ be the number of branches existing at time τ_Y^* that are descendants of node B . Each of the branches is chosen as the grafting target of the moved branch ($Y-A$) with

probability $1/G(\tau_Y^*)$. Furthermore, if the move changes the age of the root (τ_0) on the species tree, the prior on the node ages in the species tree (the τ s) will influence the proposal ratio (see equation 2 in Yang and Rannala, 2010). The factor in the proposal ratio due to the changes to the species tree is thus

$$R_{\text{Shrink}} = \frac{w_{Y^*}}{w_Y} \times \frac{0.5}{1} \times G(\tau_Y^*) \times \frac{\left(\frac{1}{0.1\tau_X^*}\right) e^{-\frac{1}{0.1\tau_X^*}(\tau_Y - \tau_X^*)}}{\frac{\lambda}{\tau_B} \left(\frac{\tau_Y^*}{\tau_B}\right)^{\lambda-1}} \times \left(\frac{\tau_Y^*}{\tau_Y}\right)^m \times \frac{g(\tau_0^*)}{g(\tau_0)} \times \left(\frac{\tau_0^*}{\tau_0}\right)^{-(s-2)}, \quad (8)$$

where m is the number of daughter nodes of A whose ages are rescaled, τ_X^* is the age of the mother node of Y^* , g is the gamma prior density for the root age τ_0 , and $s-2$ is the number of non-root interior τ nodes. The probability 0.5 is due to the sampling to choose A in the reverse Expand move. For the Expand move, the factor in the proposal ratio is $R_{\text{Expand}} = 1/R_{\text{Shrink}}$.

2. Changes to the gene trees: The gene trees are modified to avoid conflicts with the newly proposed species tree, similarly to the SPR algorithm. Some nodes are pruned off the gene tree and regrafted back and some nodes have their population IDs changed due to the disappearance and appearance of populations. In the Expand move, the target population C is ancestral to A , B , and AB (Y). In the Shrink move, the target population C is a descendent of B (see fig. 2). We scan the gene tree at each locus to identify the moved nodes. A moved node (marked with \bullet in fig. 2) has exactly one daughter node with descendants in A only. We prune off the moved node, rescale the ages inside the clade by τ_Y^*/τ_Y and re-graft it to a randomly-chosen branch that exists at the new time $t^* = t \times \frac{\tau_Y^*}{\tau_Y}$. Note that there may be multiple target gene-tree branches.

At every locus, there may be multiple moved nodes and thus multiple subtree pruning and regrafting operations on the gene trees. These are thus conducted in a disciplined manner, as follows. We prune off all moved nodes (and their attached subtrees), and “lay them on the ground”. We then determine the new ages (rescaled by τ_Y^*/τ_Y) at which the pruned subtrees are reattached, and identify and mark the reattachment points. The remaining part of the gene tree, called the skeleton, is not changed (black branches in the gene trees of fig. 2) except that gene tree nodes in population AB become nodes in population B and nodes in population C with age greater than τ_Y^* become nodes in population AC (fig. 2). We then reattach the pruned branches to the gene tree. The order of pruning and reattachment of the affected nodes is thus inconsequential. In this way we do not allow regrafting of one pruned branch onto another pruned branch, but it may be possible for a pruned branch to be regrafted to the same branch on the skeleton, so that the operation may change the node ages without changing the gene tree topology. It is also possible for multiple pruned subtrees to be reattached to the same branch of the skeleton (at different time points).

If all sequences at a locus are from populations in clade A on the species tree, all node ages on the gene tree are rescaled by τ_Y^*/τ_Y , while their population IDs remain unchanged. This rescaling is necessary as otherwise the gene tree may be in conflict with the proposed new species tree.

The changes to the gene trees will incur a factor in the proposal ratio, because the following components may not be the same in the forward and reverse moves: the number of target branches for reattaching the moved node, the probability density of the gene tree given the species tree topology and parameters τ s and θ s (i.e., the multispecies coalescent density), the rescaling of all the gene-tree node ages (by the factor τ_Y^*/τ_Y), as well as the probability of the sequence alignment given the gene tree at each locus (the phylogenetic likelihood).

In the case of only three species, the nodeslider move reduces to a variant of the general NNI algorithm for rooted trees (Yang, 2014, p.293), although it differs from the NNI algorithm implemented by Yang and Rannala (2014) or the SPR move described above. Here the nodeslider move changes both the species tree topology and a species divergence time (τ), and always changes the root of the species tree (fig. 3). In the Expand move (from $S \rightarrow S^*$ in fig. 3), branch $Y-A$ is pruned off, the age τ_Y is increased to $\tau_Y^* > \tau_X$, and the branch is reattached to the species tree, with node Y becoming the new root. The reverse Shrink move slides the root of the species tree towards the tips so that the younger node becomes the new root.

We note that each of the three moves that we have implemented to change the species tree topology, including the NNI of Yang and Rannala (2014) and the SPR and nodeslider moves of this paper, is sufficient to allow the MCMC to traverse the whole space of the species trees. In BPP, we use SPR (which includes

NNI as a special case) and nodeslider moves with pre-assigned probabilities (such as 0.6 for SPR and 0.4 for nodeslider).

Validation of the theory and implementation

The new SPR and nodeslider moves are implemented in BPP version 3.2. Our algorithms are complex and extensive testing has been conducted to confirm the correctness of the theory and the implementation. Because our new moves do not affect the calculation of the phylogenetic likelihood our tests have focused mainly on generating the prior for the species trees and parameters of the multi-species coalescent model (θ s and τ s) via MCMC when the sequence likelihood is fixed at 1. We confirmed that the SPR and nodeslider algorithms, used either alone or in combination, sampled the species trees correctly according to the prior, which is analytically available for four different priors described by Yang and Rannala (2014) and Yang (2015) for the cases of 3, 4 and 5 species.

Summary of the posterior

The BPP program generates an MCMC sample from the posterior probability distribution of species phylogenies and the posterior distribution of parameters (τ s and θ s) given each phylogeny. Here we focus on summaries of the species trees. For species tree inference the model with the highest posterior probability is presented as the maximum *a posteriori* (MAP) model. The program calculates support values for clades on the MAP tree. The program also generates posterior probabilities for individual clades as well as the majority-rule consensus tree, with support values. If the model parameters (θ s and τ s) are of primary interest we suggest that one should run the program a second time with the species tree fixed to the MAP tree or consensus tree (analysis A00, Yang, 2015). For an example see fig. 6 (below) generated by our empirical analysis of the rattlesnake dataset of Kubatko *et al.* (2011).

Results

Simulation analysis of statistical performance

Simulations were used to examine the influence on the posterior probabilities of species trees of the number of loci, the mutation rate (sequence divergence level), and the prior on topology. We simulated data under the multispecies coalescent model using either a completely symmetrical or asymmetrical tree of 16 species with two sequences sampled per species (32 sequences in total) (see fig. 4). For simplicity, we assumed equal θ s among ancestral and contemporary species with either $\theta = 0.001$ (low mutation rate) or $\theta = 0.01$ (high mutation rate). We set all internal branch lengths equal to θ , so that $\tau_i - \tau_j = \theta$ where node i is the mother of node j . Thus, the height of the root was $\tau_0 = 15 \times \theta$ for the asymmetrical tree and $\tau_0 = 4 \times \theta$ for the symmetrical tree. For each of the $2 \times 2 = 4$ parameter/topology combinations 50 datasets were simulated of either $L = 2$ or $L = 10$ unlinked loci, each with $n = 1000$ sites. Thus, $2 \times 2 \times 2 \times 50 = 400$ datasets were simulated in total. The MCcoal program which is part of the BPP package was used to generate gene trees under the multi-species coalescent model and to simulate sequence alignments on the trees under the JC69 model.

The simulated datasets were analyzed using the BPP 3.2 program with a $G(2, 200)$ prior for θ when the true $\theta = 0.01$ and a $G(2, 2000)$ prior for θ when the true $\theta = 0.001$. While the prior means match the true values, the gamma distribution with shape parameter 2 is diffuse (uninformative). Similarly, a gamma prior with shape parameter 2 and with mean equal to the true value was assigned to τ_0 , the age of the root of the species tree. In other words, the prior on τ_0 was $G(2, 50)$ for datasets simulated under a symmetrical tree with $\theta = 0.01$, $G(2, 13.3)$ for the asymmetrical tree with $\theta = 0.01$, $G(2, 500)$ for the symmetrical tree with $\theta = 0.001$, and $G(2, 133)$ for datasets simulated under an asymmetrical tree with $\theta = 0.001$. Two analyses were carried out for each dataset using different priors on the tree topology: a uniform prior on labeled histories (with rank-ordered nodes) and a uniform prior on rooted trees (ignoring node ordering).

Each of the simulated datasets (and prior combinations) were analyzed using two independent MCMC runs with different starting seeds to check convergence. Thus $400 \times 2 \times 2 = 1600$ MCMC runs were carried out in total. Each MCMC analysis was run for 200,000 iterations, sampling every second iteration and discarding the first 50,000 iterations as burn-in.

To examine the statistical performance of the method we calculated the proportion of datasets (among 50 replicate simulations) in which each of the 14 nodes in the true species tree is found in the consensus tree; note that a node of the true tree is in the consensus tree if its posterior probability is > 0.5 . This is a measure of power. We also examined the empirical coverage of the 95% and 99% Credible Set of Trees (CST). The empirical coverage is defined as the proportion of credible sets that contain the true tree. The results are summarized in Table 1. The method performs very well in identifying the true clades, even with only 2 loci. With the exception of nodes 12 to 14 at the base of the tree (see fig. 4) all nodes of the true tree are present in the consensus tree with frequencies of 0.76 or greater. The empirical coverage of the credible set of trees provides a measure of the accuracy of the method. The accuracy is very high, with the true tree contained in both the 95% and 99% credible sets of trees for 100% of simulated data analyses in all but two cases: (1) trees inferred using the uniform labeled history prior from the data simulated on an asymmetrical tree with 2 loci and with $\theta = 0.001$ – the coverage is 0.92 for the 95% and 99% CSTs; and (2) trees inferred using the uniform topology prior from the data simulated on a symmetrical tree with 2 loci and with $\theta = 0.001$ – the coverage is 0.98 for the 95% CST and 1.0 for the 99% CST. In other words, in all but one case the coverage is greater than the nominal value of either 95% or 99%.

The mean number of trees contained in the 99% CST provides a measure of the precision of the estimator of species tree topology (fig. 5 and Table 1). The mean number of trees ranged from a minimum of 1.1 (for 10 loci, $\theta = 0.01$ and a symmetrical true tree and a uniform prior on labeled histories) to a maximum of 6297.3 (for 2 loci, $\theta = 0.001$ and a symmetrical true tree with a uniform topology prior). It is evident from the mean number of trees in the CST that the prior on topology can have a large effect on the precision of the method (fig. 5 and Table 1). The uniform prior on labeled histories tends to favor symmetrical over asymmetrical trees while the uniform prior on topologies increases the probability of asymmetrical trees. When the prior favors the shape of the true tree, the estimates are more precise with a smaller CST. For example, the histograms in rows 1 and 3 of fig. 5 which represent analyses of symmetrical (Sym) trees, show an increase in the variance and mean of the number of trees in the 99% CST when using a uniform prior on rooted trees (tree) versus a uniform prior on labeled histories (LH). Conversely, the variance and mean decrease when analyzing data simulated on asymmetrical (Asym) trees as seen in rows 2 and 4 of fig. 5. In other words, the number of trees in the credible set is increased when the uniform prior on rooted trees is used to analyze data generated using a symmetrical tree. Conversely, the number of trees in the credible set is increased when a uniform labeled history prior is used to analyze data generated using an asymmetrical tree. The influence of the prior decreases when the number of loci increases from 2 to 10 and is negligible for the informative data simulated using $\theta = 0.01$ (see Table 1 and fig. 5).

Analysis of empirical datasets

The empirical dataset we analyze here includes 18 nuclear loci from six subspecies of *Sistrurus* rattlesnakes, generated and analyzed by Kubatko *et al.* (2011). Rattlesnakes are venomous snakes of the New World, with species falling into two genera: *Crotalus* which contains more than 20 species and *Sistrurus* which contains three named species: *catenatus*, *miliarius*, and *ravus*. However, mtDNA suggests that *ravus* in fact belongs to the genus *Crotalus* (Murphy *et al.*, 2002; Parkinson *et al.*, 2002). The data analyzed here are from *S. catenatus* and *S. miliarius* only. Within each of these two species, three subspecies are formally described on the basis of morphological variation in scale characters, body size and coloration, and geographic distribution. The three *S. catenatus* subspecies are *S. c. catenatus* (C), *S. c. tergeminus* (T), and *S. c. edwardsii* (E), while the three *S. miliarius* subspecies are *S. m. miliarius* (M), *S. m. barbouri* (B), and *S. m. streckeri* (S). The data also include sequences from two outgroup species: *Agkistrodon contortrix* (Ac) and *A. piscivorus* (Ap). Although the BPP analysis does not require outgroups and those two outgroup species appear quite distant from the ingroup species, we use them as well for easy comparison with the results of Kubatko *et al.* (2011).

We analyze the 18 nuclear loci and the single mitochondrial locus separately, since they have very different characterizations, including different mutation rates and effective population sizes.

Analysis of the nuclear loci: Among the 18 loci, the number of sequences per locus ranges from 48 to 52, and the sequence length ranges from 194 to 849 (Kubatko *et al.*, 2011, table 2). We use the uniform prior for rooted trees (Yang and Rannala, 2014). For the parameters on the species tree, we use the prior $\theta \sim G(2, 1000)$ with the prior mean 0.002 (2 differences per kb), and $\tau_0 \sim G(1.2, 100)$ with the prior mean for the age of the root to be 1.2%. The shape parameters (2 and 1.2) mean that the gamma priors are diffuse, while the means are chosen to be plausible for the data, based on preliminary runs of the A00 analysis (speciesdelimitation=0, speciestree=0) under a reasonable tree (Yang, 2015).

We use 8000 iterations for the burnin, after which we take 2×10^5 samples, sampling every 4 iterations. We run each analysis twice to check for consistency between runs and then merge the samples to produce summary results. Each run took about 10 hours on one CPU core. Kubatko *et al.* (2011) reported running times of ~ 10 days using StarBEAST, suggesting that the algorithms in BPP may produce better MCMC mixing properties.

We conducted two analyses. In the first, we inferred both the species delimitation and species phylogeny (A11: speciesdelimitation=1, speciestree=1). The posterior probability is 98.0% that all the six subspecies are distinct species, with 2% probability that M and B are one species. The best supported phylogeny is shown in fig. 6, and this has posterior probability 69.2%. The next two trees have different relationships for the three subspecies of *S. miliarius* (B, M, and S) from the MAP tree of fig. 6, with posterior probability 21.8% for (B, (M, S)), and posterior probability 6.3% for (M, (B, S)). Together the three trees have a cumulative posterior probability of 97.3% and constitute the 95% credibility set of models.

In the second analysis (A01: speciesdelimitation=0, speciestree=1), we treated the eight species/subspecies as distinct to infer the species tree. As in the first analysis, the top three trees differ concerning the relationships among B, M, and S, with posterior probability 69.6% for ((M, B), S) (the MAP tree of fig. 6), 23.3% for (B, (M, S)), and 6.1% for (M, (B, S)). Because the A01 analysis has a reduced model space than the A11 analysis and the shared models in the two analyses are exactly the same, the posterior probabilities for those shared models should be proportional in the two analyses.

As the 18 nuclear loci show considerable rate variation (Kubatko *et al.*, 2011, table 2), we repeated the analysis using a Gamma-Dirichlet model to account for the mutation rate variation among loci (Burgess and Yang, 2008). The gamma parameter in the model is fixed at $\alpha = 2$. This has a small effect on the parameter estimates in the A00 analysis and on the posterior probabilities on the A11 and A01 analyses. The results are summarized in table 2.

Analysis of the mitochondrial locus (ATP, 665bp): The parameters on the species tree are assigned the following priors: $\theta \sim G(2, 1000)$ with the prior mean 0.002 and $\tau_0 \sim G(1.5, 10)$ with the prior mean 0.15. All other settings are the same as for the analysis of the nuclear loci. The mitochondrial locus favoured 5 species, with M and S grouped into one species in all analyses, in contrast to the nuclear loci, which supported the distinct species status of all the 6 subspecies (Table 2). Similarly, the A01 analysis groups M and S together with posterior probability 97.7%. The A00 estimates of species divergence times (τ) are shown in figure 6c. The branches in the mitochondrial species tree are much longer than for the nuclear loci, indicating that the mitochondrial locus has a much higher mutation rate. As a result, the single mitochondrial locus appears to be at least as informative as the 18 nuclear loci.

The estimated species trees from the nuclear and mitochondrial data have strikingly different shapes. Relative to the root of the tree, the mitochondrial species tree has much older nodes for separation of *S. catenatus* and *S. miliarius*, and for the separation of the two outgroup species: *A. contortrix* and *A. piscivorus*. In the simplistic model of random mating and neutral evolution of both nuclear and mitochondrial loci, the species divergence time parameters (τ s) should be proportional for the nuclear and mitochondrial loci. The ratio of the posterior means of the species divergence times (τ s) between the mitochondrial locus and the nuclear loci is 12 for the root of the species tree, 25 for the common ancestor of *S. catenatus* and *S. miliarius*, and 24 for the divergence of the two outgroup species: *A. contortrix* and *A. piscivorus*. If the absolute species divergence times are the same for the nuclear and mitochondrial genomes, those estimates indicate that the mitochondrial mutation rate is 12-25 times as high as the nuclear mutation rate. With such mutation

rate differences and if the mitochondrial population size is $\frac{1}{4}$ that for the nuclear loci, we would expect the population size parameters on the species tree (θ s) for the mitochondrial locus to be 3 to 6 times as large as those for the nuclear loci. Yet, the average of the posterior means for θ s over the populations on the species tree is 0.0019 for the mitochondrial locus and 0.0037 for the nuclear genes, with a ratio of 0.51, while the average of the ratios is 0.81. Thus the mitochondrial θ s are far smaller than expected from the simple neutral model. In summary, both the fact that the τ estimates are not proportional between the nuclear and mitochondrial loci and the fact that the τ and θ estimates are not proportional suggest that the differences between the nuclear and mitochondrial loci cannot be entirely explained by differences in mutation rates and population sizes alone, and the idealized model does not fit the data. We suggest that extending the mitochondrial locus and sequencing more nuclear loci may be useful for understanding the major factors causing the conflicting signals.

Kubatko *et al.* (2011) conducted a number of phylogenetic and coalescent-based analyses of the same data. The coalescent-based analyses used the heuristic method STEM (Kubatko *et al.*, 2009) and the Bayesian MCMC method StarBEAST (Heled and Drummond, 2010). The 18 nuclear loci and the mitochondrial locus were analyzed as one single dataset. The species tree inferred in the StarBEAST analysis is the tree shown in figure 6c, with a posterior probability 0.93 for the M-S grouping. This may be explained by the fact that the mitochondrial locus has a much higher mutation rate so that the signal from the single mitochondrial locus has dominated the analysis when the nuclear and mitochondrial loci are analyzed together. Note that in our BPP analysis, the relationships among B, M, and S are uncertain, and the mitochondrial locus favors the M-S grouping (fig. 6c and table 2). Overall our results are largely consistent with the previous analyses of Kubatko *et al.* (2011).

Discussion

Our simulation results suggest that the full likelihood-based species tree inference method under the multi-species coalescent model, implemented in BPP, has both high precision (as indicated by the small credibility set) and high accuracy (as indicated by the high coverage probability of the credibility set). For the parameter combinations examined in our simulation, the correct species tree is recovered with high posterior probabilities when 10 loci are included in the dataset. The high power of the method is in contrast to the so-called shortcut coalescent methods which use reconstructed gene tree topologies to infer the species tree, ignoring both random and systematic errors in tree reconstruction and ignoring information in the gene tree branch lengths, leading to considerable loss of power. For example, the MPEST method (Liu *et al.*, 2010) produced many weakly supported nodes in the estimated species tree in an analysis of hundreds of loci from the genomes of mammals (Song *et al.*, 2012; Gatesy and Springer, 2013; Wu *et al.*, 2013).

We note that our current implementation has several limitations. The first is the use of the Jukes and Cantor (1969) mutation/substitution model. While this appears to be adequate when closely related species are analyzed so that the sequences are highly similar and multiple hits at the same site are uncommon, the model may not be suitable for analysis of distant species such as different orders of mammals or land plants. It should be straightforward to implement more sophisticated substitution models. The second is the assumption of the molecular clock, which is expected to be seriously violated in comparison of distantly related species. It is well-known that clock rooting of phylogenetic trees is very unreliable when the molecular clock is violated. Relaxing the molecular clock assumption in the analysis may be more challenging when the sequences are from multiple individuals of different species related through the multi-species coalescent model. Note that the relaxed clock models developed for dating species divergences are designed for species data (in which gene trees and species trees are expected to match), and modifications are needed before they can be applied to inference of species phylogenies under the multi-species coalescent model.

Software availability

The algorithms described in this paper are implemented in the program Bayesian Phylogenetics & Phylogeography (BPP) Version 3.2 which may be downloaded from <http://abacus.gene.ucl.ac.uk/software/>.

Acknowledgments

This work was supported by a Biotechnological and Biological Sciences Research Council (UK) grant (to Z.Y.). Part of this work was completed when both B.R. and Z.Y. were guests of Beijing Institute of Genomics.

References

- Bryant, D., Bouckaert, R., Felsenstein, J., Rosenberg, N. A., and RoyChoudhury, A. 2012. Inferring species trees directly from biallelic genetic markers: bypassing gene trees in a full coalescent analysis. *Mol Biol Evol*, 29(8): 1917–1932.
- Burgess, R. and Yang, Z. 2008. Estimation of hominoid ancestral population sizes under Bayesian coalescent models incorporating mutation rate variation and sequencing errors. *Mol Biol Evol*, 25(9): 1979–1994.
- Degnan, J. H. and Rosenberg, N. A. 2006. Discordance of species trees with their most likely gene trees. *PLoS Genet*, 2(5): e68.
- Degnan, J. H. and Salter, L. A. 2005. Gene tree distributions under the coalescent process. *Evolution*, 59(1): 24–37.
- Edwards, S. V. 2009. Is a new and general theory of molecular systematics emerging? *Evolution*, 63(1): 1–19.
- Edwards, S. V., Liu, L., and Pearl, D. K. 2007. High-resolution species trees without concatenation. *Proc Natl Acad Sci USA*, 104(14): 5936–5941.
- Felsenstein, J. 1981. Evolutionary trees from dna sequences: a maximum likelihood approach. *J Mol Evol*, 17(6): 368–376.
- Gatesy, J. and Springer, M. S. 2013. Concatenation versus coalescence versus “concatalescence”. *Proc Natl Acad Sci USA*, 110(13): E1179–E1179.
- Heled, J. and Drummond, A. J. 2010. Bayesian inference of species trees from multilocus data. *Mol Biol Evol*, 27(3): 570–580.
- Jukes, T. H. and Cantor, C. R. 1969. Evolution of protein molecules. *Mammalian Protein Metabolism*, 3: 21–132.
- Kubatko, L. S. and Degnan, J. H. 2007. Inconsistency of phylogenetic estimates from concatenated data under coalescence. *Syst Biol*, 56(1): 17–24.
- Kubatko, L. S., Carstens, B. C., and Knowles, L. L. 2009. Stem: species tree estimation using maximum likelihood for gene trees under coalescence. *Bioinformatics*, 25(7): 971–973.
- Kubatko, L. S., Gibbs, H. L., and Bloomquist, E. W. 2011. Inferring species-level phylogenies and taxonomic distinctiveness using multilocus data in *Sistrurus rattlesnakes*. *Syst Biol*, 60(4): 393–409.
- Leaché, A. D. and Rannala, B. 2011. The accuracy of species tree estimation under simulation: a comparison of methods. *Syst Biol*, 60(2): 126–137.
- Liu, L., Yu, L., Pearl, D. K., and Edwards, S. V. 2009. Estimating species phylogenies using coalescence times among sequences. *Syst Biol*, 58: 468–477.
- Liu, L., Yu, L., and V., E. S. 2010. A maximum pseudo-likelihood approach for estimating species trees under the coalescent model. *BMC Evol Biol*, 10(3): 302.
- Maddison, W. P. 1997. Gene trees in species trees. *Syst Biol*, 46: 523–536.
- Maddison, W. P. and Knowles, L. L. 2006. Inferring phylogeny despite incomplete lineage sorting. *Syst Biol*, 55(1): 21–30.
- Mossel, E. and Roch, S. 2010. Incomplete lineage sorting: consistent phylogeny estimation from multiple loci. *IEEE/ACM Trans Computat Biol Bioinform (TCBB)*, 7(1): 166–171.

- Murphy, R. W., Fu, J., Lathrop, A., Feltham, J. V., and Kovac, V. 2002. Phylogeny of the rattlesnakes (*Crotalus* and *Sistrurus*) inferred from sequences of five mitochondrial DNA genes. In G. W. Schuett, M. Hoggren, M. E. Douglas, and H. W. Greene, editors, *Biology of the Vipers*, pages 69–92. Eagle Mountain Publishing, Eagle Mountain, Utah, USA.
- Page, R. D. and Charleston, M. A. 1997. From gene to organismal phylogeny: reconciled trees and the gene tree/species tree problem. *Mol Phylogenet Evol*, 7: 231–240.
- Parkinson, C. L., Campbell, J. A., Chippindale, P. T., and Schuett, G. 2002. Multigene analyses of pitviper phylogeny with comments on their biogeographical history. In G. W. Schuett, M. Hoggren, M. E. Douglas, and H. W. Greene, editors, *Biology of the Vipers*, pages 93–110. Eagle Mountain Publishing, Eagle Mountain, Utah, USA.
- Rannala, B. and Yang, Z. 2003. Bayes estimation of species divergence times and ancestral population sizes using DNA sequences from multiple loci. *Genetics*, 164(4): 1645–1656.
- Rannala, B. and Yang, Z. 2008. Phylogenetic inference using whole genomes. *Annu Rev Genomics Hum Genet*, 9: 217–231.
- Rannala, B. and Yang, Z. 2013. Improved reversible jump algorithms for Bayesian species delimitation. *Genetics*, 194: 245–253.
- Ronquist, F., Teslenko, M., van der Mark, P., Ayres, D. L., Darling, A., Höhna, S., Larget, B., Liu, L., Suchard, M. A., and Huelsenbeck, J. P. 2012. MrBayes 3.2: Efficient Bayesian phylogenetic inference and model choice across a large model space. *Syst Biol*, 61(3): 539–542.
- Song, S., Liu, L., Edwards, S. V., and Wu, S. 2012. Resolving conflict in eutherian mammal phylogeny using phylogenomics and the multispecies coalescent model. *Proc Natl Acad Sci USA*, 109(37): 14942–14947.
- Wu, S., Song, S., Liu, L., and Edwards, S. V. 2013. Reply to Gatesy and Springer: The multispecies coalescent model can effectively handle recombination and gene tree heterogeneity. *Proc Natl Acad Sci USA*, 110(13): E1180–E1180.
- Yang, Z. 2002. Likelihood and Bayes estimation of ancestral population sizes in hominoids using data from multiple loci. *Genetics*, 162(4): 1811–1823.
- Yang, Z. 2014. *Molecular Evolution: A Statistical Approach*. Oxford University Press, Oxford, England.
- Yang, Z. 2015. The bpp program for species tree estimation and species delimitation. *Curr Zool*, 61: 854–865.
- Yang, Z. and Rannala, B. 2010. Bayesian species delimitation using multilocus sequence data. *Proc Natl Acad Sci USA*, 107: 9264–9269.
- Yang, Z. and Rannala, B. 2014. Unguided species delimitation using DNA sequence data from multiple loci. *Mol Biol Evol*, 31(12): 3125–3135.

Table 1: Summary of results for simulation analyses.

		Number of loci: 2				Number of loci: 10				
		Symmetrical tree		Asymmetrical tree		Symmetrical tree		Asymmetrical tree		
		$\theta = 0.01$	$\theta = 0.001$	$\theta = 0.01$	$\theta = 0.001$	$\theta = 0.01$	$\theta = 0.001$	$\theta = 0.01$	$\theta = 0.001$	
Prior	LH	T	LH	T	LH	T	LH	T	LH	T
Proportion of datasets with true node present in consensus tree										
Node										
1	.98	.98	.80	.76	.98	1.0	.88	.86	1.0	1.0
2	1.0	.98	.90	.84	.94	.96	.88	.90	1.0	1.0
3	1.0	1.0	.88	.74	.98	1.0	.84	.86	1.0	1.0
4	.98	.94	.92	.92	.96	1.0	.82	.84	1.0	1.0
5	.96	.92	.90	.88	.94	.98	.76	.80	1.0	1.0
6	1.0	1.0	.90	.80	.96	.98	.78	.84	1.0	1.0
7	.96	.96	.76	.64	.96	.98	.76	.80	1.0	1.0
8	1.0	.98	.88	.82	.96	1.0	.84	.86	1.0	1.0
9	.98	.98	.90	.90	.94	.98	.86	.88	1.0	1.0
10	.96	.96	.80	.78	.98	1.0	.86	.90	1.0	1.0
11	.98	.94	.80	.76	.96	1.0	.76	.80	1.0	1.0
12	.98	.96	.92	.88	.90	.96	.68	.80	1.0	1.0
13	.96	.96	.76	.68	.86	.94	.36	.64	1.0	1.0
14	.96	.94	.78	.74	.66	.80	.13	.46	1.0	1.0
CST							Empirical coverage			
95 %	1.0	1.0	1.0	.98	1.0	1.0	.92	1.0	1.0	1.0
99 %	1.0	1.0	1.0	1.0	1.0	1.0	.92	1.0	1.0	1.0
CST							Mean number of trees in 99% CST			
	243.5	372.8	4375.7	6297.3	443.9	200.9	6205.8	2711.7	1.1	1.1
							15.6	19.1	3.7	3.0
							46.9	26.3		

The upper matrix shows the proportion of simulated datasets for which each node of the true species tree is present in consensus tree. The empirical coverage of the 95% and 99% credible sets of trees (CSTs) tabulates the proportion of simulated datasets (across 50 simulated datasets for each set of simulation conditions) for which the true tree is contained within the credible set. The mean number of trees in the CST is the average number of trees in the 99% CST (averaging across 50 simulated datasets for each set of simulation conditions). Note – each dataset is analyzed using two species tree priors: the uniform prior for labeled histories (LH) and the uniform prior for rooted trees (T). Node numbers are shown in fig. 4.

Table 2: Summary of results obtained from BPP analysis of the rattlesnake datasets.

	28 nuc loci, one rate	28 nuc loci, gamma rate G(2)	ATP (665bp)
	$\tau_0 \sim G(1.2, 100)$	$\tau_0 \sim G(1.2, 100)$	$\tau_0 \sim G(1.5, 10)$
	$\theta_0 \sim G(2, 1000)$	$\theta_0 \sim G(2, 1000)$	$\theta_0 \sim G(2, 1000)$
A00 estimates			
τ_0 (root)	0.0125 (0.0097, 0.0154)	0.0139 (0.0100, 0.0172)	0.145 (0.127, 0.164)
τ_1 (CET-SMB)	0.0042 (0.0033, 0.0052)	0.0044 (0.0034, 0.0054)	0.106 (0.088, 0.124)
τ_2 outgroup	0.0026(0.0013, 0.0039)	0.0026 (0.0014, 0.0039)	0.062 (0.047, 0.077)
A11 analysis			
Pr(MS)	0.000	0.000	0.968
Pr(MB)	0.020	0.015	0.000
Pr(ET)	0.000	0.000	0.335
P_4	0.000	0.000	0.330
P_5	0.020	0.015	0.652
P_6	0.980	0.985	0.018
A01 analysis			
(MB)-S	0.696	0.608	0.013
(MS)-B	0.232	0.313	0.977
(BS)-M	0.061	0.071	0.011

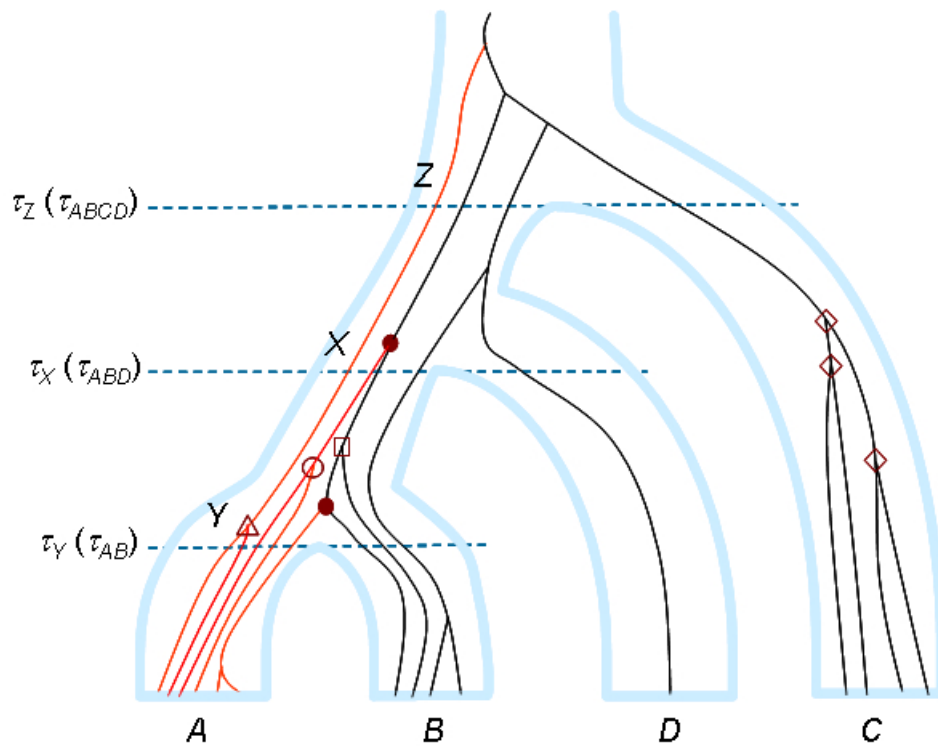


Figure 1: The SPR move removes branch Y-A on the species tree (with the clade A) and reattaches it to a target branch C, while changing the gene trees through similar SPR moves to prevent conflicts between the newly proposed species tree and the gene trees. Moved nodes on the gene tree, marked as ●, have exactly one daughter node with descendants in A only. The species tree is represented by the light blue boundary pipes while the gene tree is represented by lines contained within the species tree. This is the case with species $AB(Y)$ or the species on the path from Y to Z (the common ancestor of A and C). Moved nodes are pruned and regrafted to a randomly chosen branch in a species on the path from C to Z. Other affected nodes, marked by ○, △ or □, have their population IDs changed by the move.

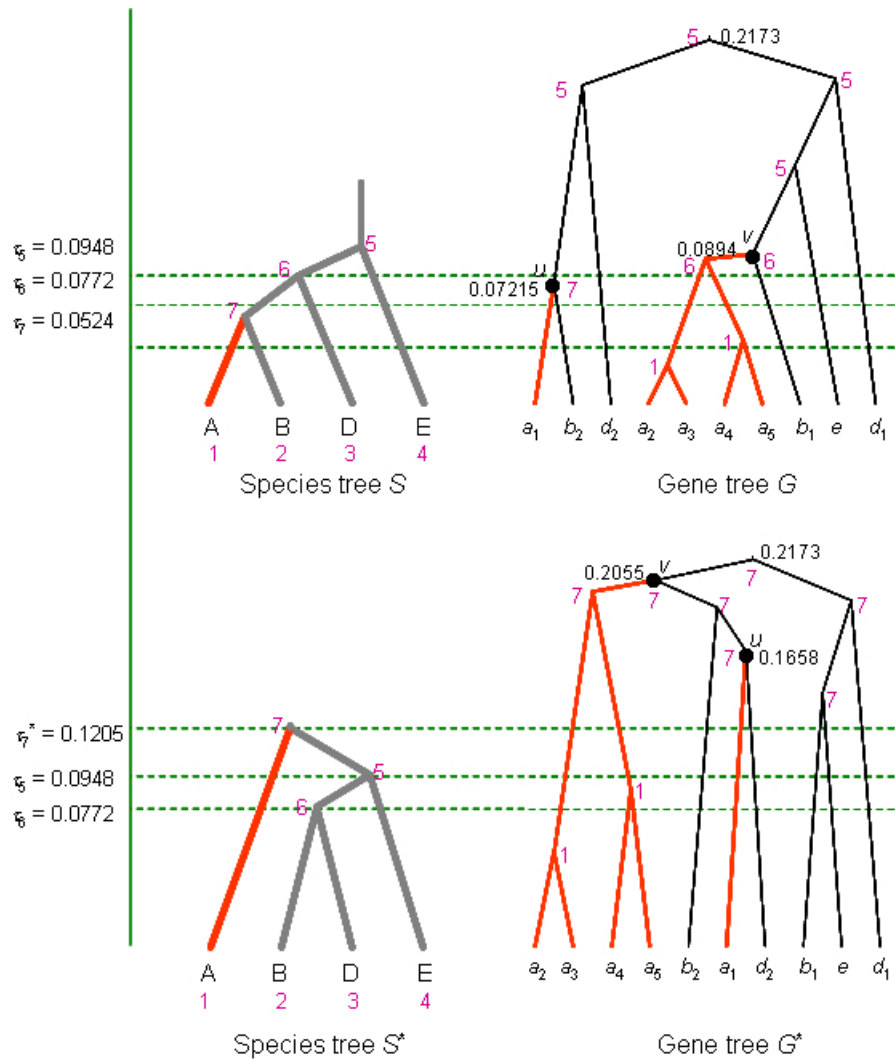


Figure 2: The nodeslider move prunes branch $Y-A$ on the species tree (with clade A), changes the age of Y (τ_Y), rescales the ages of nodes inside A by the factor τ_Y^*/τ_Y , and reattaches the branch to the species tree either at a branch ancestral to Y (if $\tau_Y^* > \tau_Y$, Expand move) or at a branch that is descendent to B (if $\tau_Y^* < \tau_Y$, Shrink move). Ages of nodes in the affected clades on the gene trees are scaled by the same factor τ_Y^*/τ_Y .

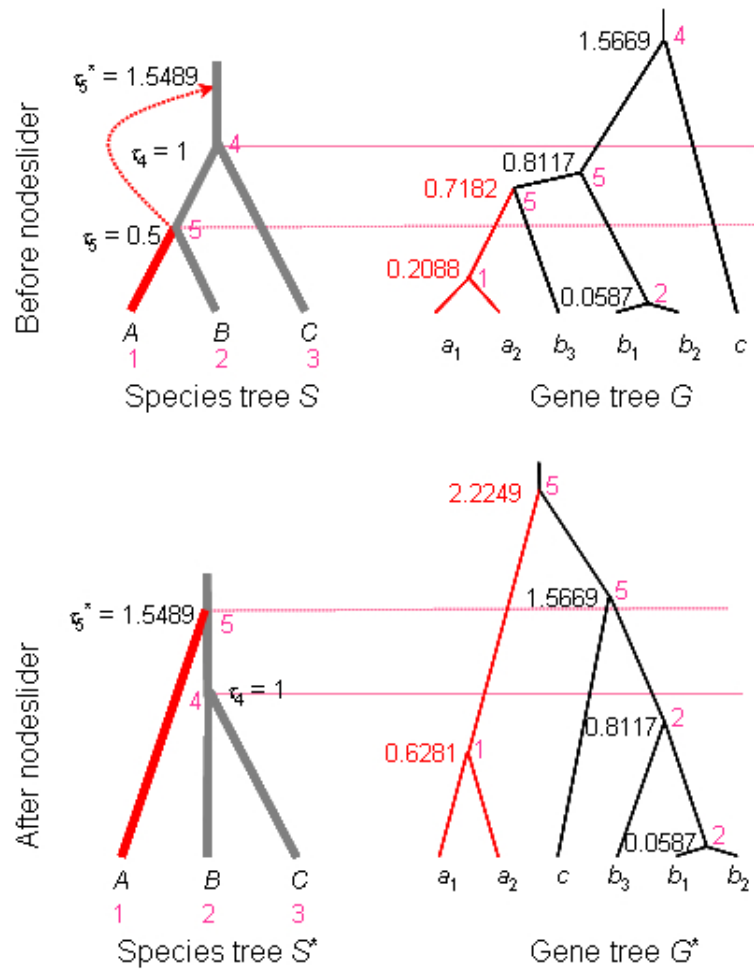


Figure 3: The nodeslider move for 3 species is a variant of the NNI rearrangement for rooted trees, which changes both the species tree topology and a species divergence time (τ), and always changes the root of the species tree.

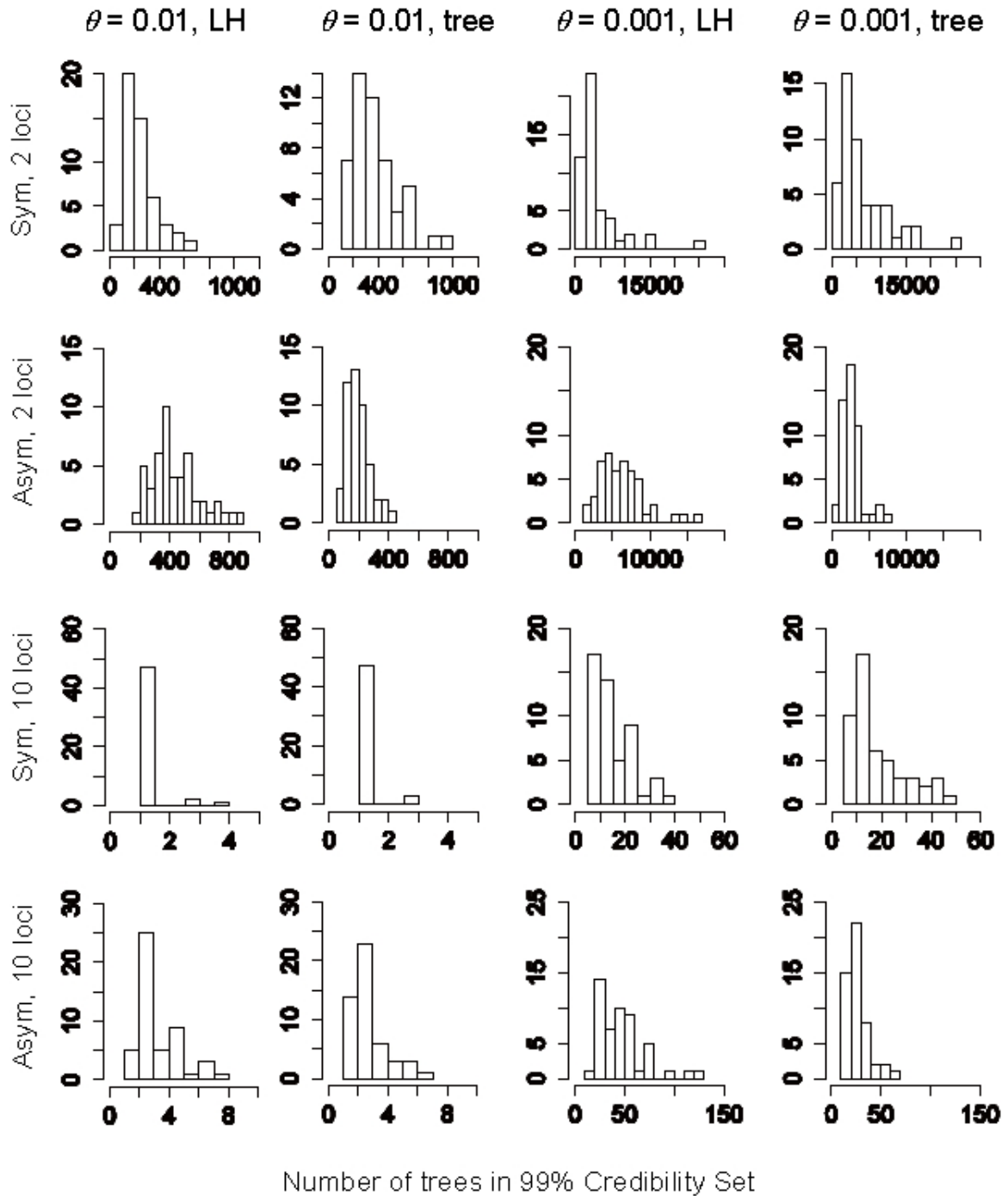


Figure 5: Frequency distributions of the number of trees contained in the 99% credible sets from analyses of 50 simulated datasets for each of 8 combinations of simulation conditions and two different topology priors: LH=labeled history (columns 1 and 3); tree=topology (columns 2 and 4). The upper two rows show results for two loci and the lower two rows results for 10 loci. Rows 1 and 3 are results for data simulated on symmetrical (Sym) trees and rows 2 and 4 for asymmetrical (Asym) trees. The two columns to the left are simulations using $\theta = 0.01$ and the two columns on the right are those using $\theta = 0.001$

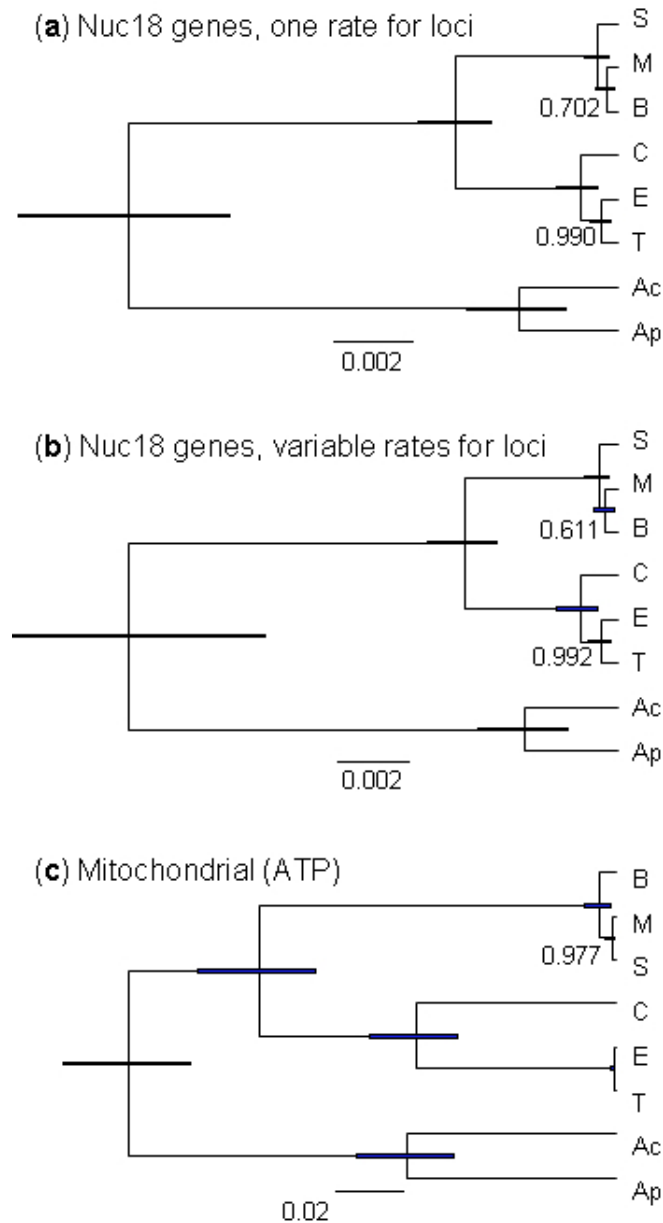


Figure 6: The MAP trees for the six subspecies of *Sistrurus* rattlesnakes and the outgroups in three different analyses of the nuclear (18 loci) and mitochondrial datasets. The three *S. catenatus* subspecies are *S. c. catenatus* (C), *S. c. tergeminus* (T), and *S. c. edwardsii* (E), while the three *S. miliarius* subspecies are *S. m. miliarius* (M), *S. m. barbouri* (B), and *S. m. streckeri* (S). The numbers next to the internal nodes are the posterior probabilities for the clades in the species tree (analysis A01: speciesdelimitation = 0, speciestree = 1). The branch lengths are drawn to represent the posterior means of the divergence times (τ s) in the A00 analysis (speciesdelimitation = 0, speciestree = 0), with the phylogeny fixed, while the node bars represent the 95% HPD interval.